Coexisting attractors in periodically modulated logistic maps

Thounaojam Umeshkanta Singh, Amitabha Nandi, and Ram Ramaswamy
School of Physical Sciences, Jawaharlal Nehru University, New Delhi 110 067, India
(Received 12 November 2007; published 23 June 2008)

We consider the logistic map wherein the nonlinearity parameter is periodically modulated. For low periods, there is multistability, namely two or more distinct dynamical attractors coexist. The case of period 2 is treated in detail, and it is shown how an extension of the kneading theory for one-dimensional maps can be applied in order to analyze the origin of bistability, and to demarcate the principal regions of bistability in the phase space. When the period of the modulation is increased—and here we choose periods which are the Fibonacci numbers—the measure of multistable regions decreases. The limit of quasiperiodic driving is approached in two different ways, by increasing the period and keeping the drive dichotomous, or by increasing the period and varying the modulation sinusoidally. In the former case, we find that multistability persists in small regions of the phase space, while in the latter, there is no evidence of multistability but strange nonchaotic attractors are created.

DOI: 10.1103/PhysRevE.77.066217 PACS number(s): 05.45.−a

I. INTRODUCTION

Parametric modulation has been an important technique in nonlinear control strategies, and has been studied extensively in the past few decades [1,2]. Periodic, aperiodic, and quasiperiodic variation of the parameters of typical nonlinear systems have been shown to result in bifurcations and dynamical transitions [3]. In driven dissipative systems, the dynamics is asymptotically on attractors on which the motion can be chaotic or nonchaotic. The effect of quasiperiodic driving on nonlinear dynamical systems has been studied in detail [4–7], and it is known that the dynamics can be on nonchaotic attractors having a fractal geometry.

Another important phenomena which has been frequently observed in the parametric modulated system, is that of bistability (or multistability) where two (or several) attractors can simultaneously coexist in the phase space at a given set of parameter values. Autonomous systems with multiple steady states are well known, and examples can be drawn from nonlinear optics [8], nonlinear electronic circuits [9], ecological [10] or biological systems [11–13]. Multistability is an advantage—and indeed a desirable feature—in systems with potential applications to pattern recognition or in memory storage devices [14,15]. On the other hand, in situations where it is required that a system respond reliably in a specific dynamical state multistability can be undesirable: From a practical point of view multistability can be disadvantageous since it often severely delimits the operating regimes of those systems [16].

Modulation can play an effective role in inducing [17] or destroying multistability [18]. Multiple coexisting periodic attractors—the phenomenon of generalized multistability—has been observed experimentally in the CO_2 laser [19]. In the context of biology, switching between stable steady states in response to external stimuli is known to play a crucial role in cell signaling [11], cell differentiation [12] or gene regulation [13]. Modulation can arise through coupling to internal circadian or ultradian oscillators, and thus the study of how multistability arises and vanishes in modulated nonlinear systems can provide a framework for understanding the operation of natural biological switches [20].

The model that we study here is a modulated logistic mapping [3] where the nonlinearity parameter varies with iteration step, namely

$$x_{n+1} = r_n x_n (1 - x_n). \tag{1}$$

Our motivation is to examine the occurrence of multistability, and to study its dependence on the period of modulation. To that end we consider two different sequences of periodic modulation with the periods chosen to be the Fibonacci numbers, $F_k = F_{k-1} + F_{k-2}$, $F_{-1} = 0$, $F_0 = 1$.

The first instance is that of dichotomous modulation: r_n can take one of two values, $r_+ = r + \varepsilon$ or $r_- = r - \varepsilon$, and the sequence of the r_n's has period F_k [21]. In the second case, the modulation is taken to be sinusoidal, $r_n = r + \varepsilon \cos 2\pi n \omega_k$, with $\omega_k = F_{k-1}/F_k$. As $k \to \infty$, the modulation becomes quasiperiodic.

Both forms are identical for $k=2$, namely the case of period-2 modulation when $r_n = r + (-1)^n \varepsilon$ [22] and this case is examined in some detail. The conditions for the multistability and the corresponding regions in phase space can be analyzed via an extension of the kneading theory for one-dimensional (1D) maps [23]. Complete knowledge of the occurrence of periodic windows and their fundamental structure in parameter space is important from the point of view of control as well as experimental design [24] and we show how this can be done in the present instance by extending and adapting the analysis introduced by Metropolis, Stein, and Stein [25]. This analysis [26] is presented in Sec. II of the paper.

We consider the case of higher period drives in Sec. III, and see that bistable regions continue to exist, though with varying extent in the phase space. The boundaries of these regions can be deduced in a fairly straightforward manner, keeping in mind that the system is effectively of dimension F_k.

The quasiperiodic limit is considered in Sec. IV. As is known from a number of previous studies, for sinusoidal driving, the quasiperiodically driven logistic map supports strange nonchaotic dynamics [5]. In this case there is no multistability. On the other hand, we find that multistability

persists in the case of the dichotomous drive. The paper concludes with a summary and discussion in Sec. V.

II. PERIODIC MODULATION OF THE LOGISTIC MAP

The modulated systems that we consider here can be written in the general form

$$x_{n+1} = [r + \varepsilon g(\theta_n)]x_n(1 - x_n), \tag{2}$$

$$\theta_{n+1} = \theta_n + \omega_k, \quad \text{mod } 1, \tag{3}$$

where $\omega_k = F_{k-1}/F_k$, the ratio of successive Fibonacci numbers, is a rational number. In the limit $k \to \infty$, $\omega_k \to (\sqrt{5} - 1)/2$, the inverse golden mean ratio. For definiteness we take the initial "phase" $\theta_0 = 0$.

For the case of sinusoidal modulation we take

$$g(\theta_n) = \cos(2\pi\theta_n), \tag{4}$$

while the function

$$g(\theta_n) = 1 - 2\Theta(\theta_n - \omega), \tag{5}$$

gives the periodic dichotomous modulation [where $\Theta(\cdots)$ is the Heaviside function].

Period 1 is "un"modulation: When $k=1$, $\omega_1 = 1$ and $g(\theta) = 1$ is constant for all n. When $k=2$, both forms of the forcing are effectively identical and the function g can be written as the sequence

$$\{g\} = \{+1, -1, +1, -1, \ldots\}.$$

This case can be reduced to the study of a combination of two separate mappings, as we discuss below.

Period-2 forcing. The case of period-2 modulation

$$x_{n+1} = (r + \varepsilon \cos \pi n)x_n(1 - x_n) \tag{6}$$

can be treated as a combination of the maps [22]

$$f_{\pm}(x_n) \equiv (r \pm \varepsilon)x_n(1 - x_n), \tag{7}$$

with

$$x_{n+1} = f_+(x_n), \quad x_{n+2} = f_-(x_{n+1}). \tag{8}$$

The maps $f_{2\alpha}$ and $f_{2\beta}$, which are obtained by alternate applications of the maps f_+ and f_-,

$$f_{2\alpha} = f_- \circ f_+, \quad f_{2\beta} = f_+ \circ f_- \tag{9}$$

are topologically conjugate since f_+ and f_- are locally invertible [22]

$$f_{2\alpha} = f_+^{-1} \circ f_{2\beta} \circ f_+ \tag{10}$$

and

$$f_{2\beta} = f_-^{-1} \circ f_{2\alpha} \circ f_-. \tag{11}$$

This implies that the kneading sequences of $f_{2\alpha}$ and $f_{2\beta}$ are identical [27].

For nonzero ε, the attractors of $f_{2\alpha}$ (or $f_{2\beta}$) are not complementary, and the possibility of bistability arises [22] (for period 2 there can be at maximum two coexisting attractors).

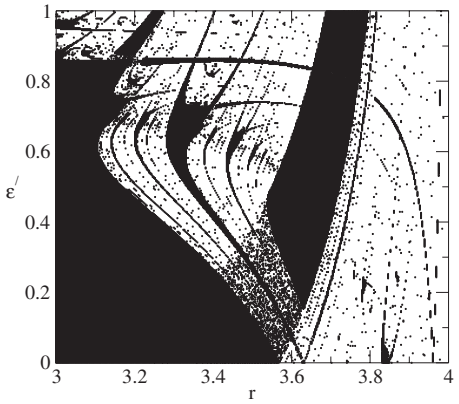

FIG. 1. Dynamics in the r, ε' plane with period-2 modulation. The black regions correspond to the periodic dynamics and the white regions correspond to the chaotic dynamics. For a particular r, with $\varepsilon' > 1$, there could be stable dynamical behavior, but those regions are not considered in the present study.

To study the global nature of dynamics, we obtain the phase diagram for the system as a function of the parameters r and nonzero ε. We examine the behavior of typical orbits of Eq. (6) and Eq. (7) as a function of these parameters.

To keep the dynamics globally bounded, we rescale Eq. (6) [and similarly Eq. (7)],

$$x_{n+1} = [r + (4 - r)\varepsilon' \cos \pi n]x_n(1 - x_n), \tag{12}$$

in the parameter regime $0 \le \varepsilon' \le 1$. There can be bounded motion for $\varepsilon' > 1$, but in the present study we do not consider this region here, as also the case of negative ε'. Figure 1 shows the regions of stable periodic and chaotic motion in the (r, ε') plane. This is done by computing the nontrivial Lyapunov exponent given by

$$\lambda = \lim_{N \to \infty} \frac{1}{N} \sum_{i=1}^{N} \ln \left| \frac{\partial x_{i+1}}{\partial x_i} \right|, \tag{13}$$

which is positive for chaotic motion and negative for periodic motion.

As in our previous work [26], here also we observe regions having the characteristic and canonical shape of "swallows" or "shrimps." This has also been observed before for a class of two-parameter maps [24,28,29]. These stable regions occur around superstable orbits [26,29], which we will discuss in the next section.

Along the axis $\varepsilon' = 0$, the system is merely the logistic map, $x \to rx(1-x) \equiv f(x)$. Because the modulation has period 2, for nonzero ε' the odd n orbits of the logistic map become period-$2n$ orbits.

(1) *Bistability with period-2 forcing*. The polynomial $f_{2\alpha}(x)$ is quartic, and there can therefore be 0, 2 or 4 fixed points. We study the dynamics by computing the Lyapunov exponents for different initial conditions and as shown in Fig. 2(a), for appropriate values of ε' there can be bistability, namely two distinct attractors with different Lyapunov exponents.

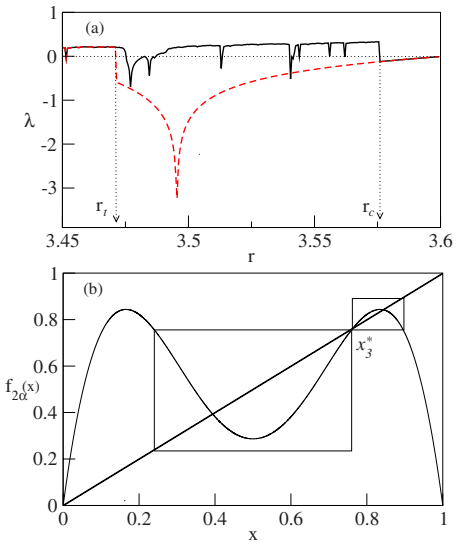

FIG. 2. (Color online) (a) The variation of Lyapunov exponents for different initial conditions as a function of the nonlinearity parameter r along the line $\varepsilon'=0.386\,944$. At $r_t\approx 3.471$, there is a tangent bifurcation that results in the creation of two coexisting attractors. Bistability persists until the crisis at $r_c\approx 3.576$ when trajectories of the chaotic attractor intrude into the basin of periodic attractor. (b) Return map of $f_{2\alpha}(x)$ at $r=3.5$ and $\varepsilon'=0.25$. Trajectories that start within one of the boxes clearly remain within that box: Thus there is bistability.

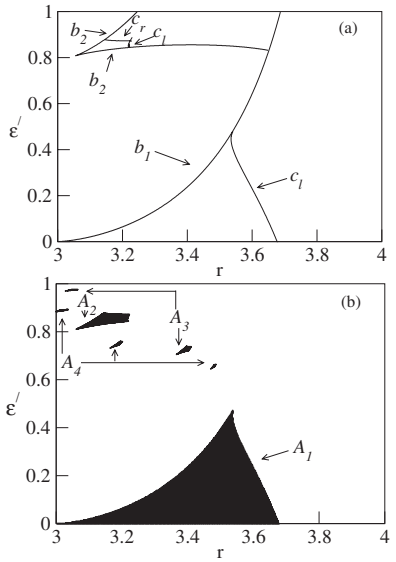

FIG. 3. (a) Boundaries of bistability regions A_1 and A_2 [as shown in (b)]. The curve b_1 divides the parameter space into regions of 2 and 4 fixed-point regions of $f_{2\alpha}(x)$. The crisis line c_l of the left-hand attractor meets with b_1 and the region between the inside of these curves gives the bistability region. Similarly, the b_2 line dividing 4 and 8 fixed point regions of $f_{2\alpha}^2(x)$ intersect with crisis curve c_l and c_r of the left-hand and right-hand attractors to give regions of bistability arising from $f_{2\alpha}^2(x)$. (b) Bistability regions (black) in the (r,ε') plane. A_1, A_2, and A_3 corresponds to regions of coexisting attractors contributing from $f_{2\alpha}(x)$, $f_{2\alpha}^2(x)$, $f_{2\alpha}^3(x)$, and $f_{2\alpha}^4(x)$, respectively.

For low ε', the system has two fixed points for small r and all trajectories are attracted to the basin of the stable attractor x_2^* (the subscript is an ordinal index, counting outwards from the origin). At $r=r_t$, there is a tangent bifurcation creating the fixed point x_3^* which is unstable and x_4^* which is stable. The two stable attractors x_2^* and x_4^* are not complementary [22]; the dynamics is effectively governed by the combination mapping, $f_{2\alpha}$ which has three critical points, $x_a=\frac{1}{2}$ and

$$x_{b,c}=\frac{1}{2}\pm\frac{\sqrt{1-2(r-\varepsilon)^{-1}}}{2}, \tag{14}$$

given by the condition $f'_{2\alpha}(x)=0$. For a general first-order difference equation, the maximum number of coexisting attractors is equal to the number of critical points [30]. Singer [27,31] further showed that a sufficient condition for these attractors to be stable is that the Schwarzian derivative

$$Sf(x)=\frac{f'''(x)}{f'(x)}-\frac{3}{2}\left(\frac{f''(x)}{f'(x)}\right)^2 \tag{15}$$

is negative. This condition holds for $f_{2\alpha}$, and thus it turns out that there are at most two stable attractors [22,30]. The critical points x_b and x_c are symmetric about x_a, and the bounding boxes about the unstable fixed point x_3^* is shown in Fig. 2(b). If points that start inside a given box stay within the box, there can clearly be two coexisting attractors or bistability. The dynamics can be periodic or chaotic on the two attractors.

Bistability ends at $r=r_c$ when the attractors merge in a transfer crisis [26,32,33]; chaotic trajectories of one of the attractors escape from its bounding box and intrude into the basin of the other [see Fig. 2(a)]. Shown in Fig. 3(a) is the curve b_1 which is a line of tangent bifurcations that divides parameter space into regions of 2 or 4 fixed points of $f_{2\alpha}(x)$. In the region A_1, the condition for bistability is that the following conditions hold simultaneously:

$$f_{2\alpha}^2(x_a)\le x_3^*,\quad f_{2\alpha}^2(x_b)\ge x_3^*. \tag{16}$$

Similarly there can be higher order bistable regions. For $f_{2\alpha}^2(x)$, there can be regions of four fixed points, two stable and two unstable. The curve b_2 divides parameter space into regions of four and eight fixed point regions of $f_{2\alpha}^2(x)$. Following the argument given above for identifying the region A_1, the curves c_l or c_r that define the crises of the left and right attractors, respectively, bound the region of bistability denoted A_2 in Fig. 3(b). Higher iterates give rise to still more regions of bistability although these regions shrink in area and become less observable.

In the pth iterate of the map, there are p tangent bifurcations simultaneously and two attractors continue to coexist as long as the local critical points of the map are "boxable" about newly created p unstable fixed points (cf. Table I). Since the unstable point x_3^* (which is the third fixed point from the origin) is common to every iterate of the map, the bistability region arising from the pth composition of the map, $f_{2\alpha}^p(x)$, is given via the conditions

TABLE I. Characterization of bistable regions for period-2 modulation.

Iterates p	Unstable fixed point	Number of bistable region	Boundary
1	x_3^*	1 in 4 fixed point region	(i) Boundary of regions of 2 and 4 fixed points (ii) $c_l=x_3^*-f_{2\alpha}^2(x_{cl})=0$ [a] (iii) $\varepsilon'=0$
2	x_3^*,x_7^*	1 in 8 fixed point region	(i) Boundary of regions of 4 and 8 fixed points (ii) $c_l=x_3^*-f_{2\alpha}^4(x_{cl})=0$ (iii) $c_r=f_{2\alpha}^4(x_{cr})-x_3^*=0$ [b]
3	x_3^*,x_7^*,x_{13}^*	2 in 14 fixed point region	(i) Boundary of regions of 8 and 14 fixed points (ii) $c_l=x_3^*-f_{2\alpha}^6(x_{cl})=0$ (iii) $c_r=f_{2\alpha}^6(x_{cr})-x_3^*=0$
4	$x_3^*,x_7^*,x_{11}^*,x_{15}^*$	2 in 16 fixed point region	(i) Boundary of regions of 8 and 16 fixed points (ii) $c_l=x_3^*-f_{2\alpha}^8(x_{cl})=0$ (iii) $c_r=f_{2\alpha}^8(x_{cr})-x_3^*=0$
	$x_3^*,x_7^*,x_{13}^*,x_{23}^*$	1 in 24 fixed point region	(i) Boundary of regions of 16 and 24 fixed points (ii) $c_l=x_3^*-f_{2\alpha}^8(x_{cl})=0$ (iii) $c_r=f_{2\alpha}^8(x_{cr})-x_3^*=0$

[a] c_l=Crisis curve of attractor to the left of x_3^*.
[b] c_r=Crisis curve of attractor to the right of x_3^*.

$$f_{2\alpha}^{2p}(x_{cl}) \le x_3^*, \quad f_{2\alpha}^{2p}(x_{cr}) \ge x_3^*, \tag{17}$$

where x_{cl} and x_{cr} are left-hand and right-hand critical points about x_3^*.

(2) *One-dimensional analysis*. Although at alternate time steps the dynamics evolves according to the mappings f_+ and f_-, respectively, it is possible to extend the algebraic analysis of the itineraries of superstable orbits as introduced by Metropolis, Stein, and Stein [25]. The extended MSS algebra (or U sequences) gives a total description of the organization of the periodic orbits in the parameter space [26] by attaching subscripts plus (+) and minus (−) (depending on which of the mappings $f_\pm$ is used) to the symbols R, L, and C, which denote [25] whether the map iterate is to the right or left of the center (the map maximum).

A periodic orbit of even period k is determined by the condition

$$f_{s_1\cdots s_k}^{(k)}(x) \equiv f_{s_k}(f_{s_1\cdots s_{k-1}}^{(k-1)}(x)) = x, \tag{18}$$

where $s_1 s_2 \cdots s_k$ is an alternating sequence of plus and minus. Many of these are extensions of even period orbits which exist in the unmodulated logistic map, namely for $\varepsilon'=0$, and are stable when

$$\mu = \left| \prod_{i=1}^{k} f'_{s_i}(x_i) \right| < 1. \tag{19}$$

Superstable orbits, those where the critical point of either f_- or f_+ belong to the orbit, have valid itineraries that are given by extending the MSS sequences [25]. The condition for superstability is met along a line (namely codimension 1) in the $(r-\varepsilon')$ parameter plane: These are denoted M_j^k in Fig. 4, the subscript j indexing the several different such orbits that can occur. Doubly superstable (DSS) orbits occur at points in the parameter plane since two conditions—that the critical points of both $f+$ and f_- are elements of the orbit—must be met. One such point is indicated.

Odd period orbits do not occur in this system. Consider the superstable period-3 orbit which has the itinerary CRL in the unmodulated logistic map. This gives rise to two different period-6 orbits, $\hat{M}_1^6 \equiv \mathrm{C\_R_+L\_R_+R\_L_+}$ and $\hat{M}_2^6 \equiv \mathrm{C\_R_+L\_L_+R\_L_+}$ in the present case.

The period-6 orbits in the logistic map, which has itineraries $\mathrm{CRLR^3}$ and $\mathrm{CRL^2R^2}$, here becomes $M_1^6 \equiv \mathrm{C_+R\_L_+R\_R_+R\_}$ and $M_2^6 \equiv \mathrm{C_+R\_L_+L\_R_+R\_}$, respectively.

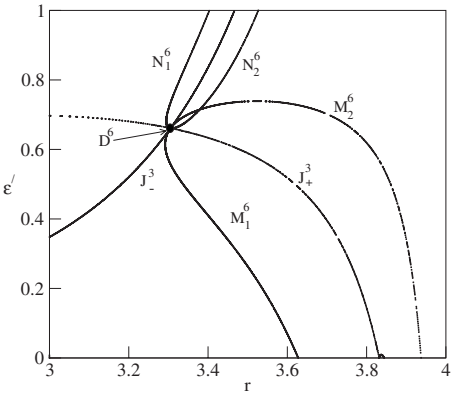

FIG. 4. Lines of the superstable orbits in parameter space. Only even periodic orbits are present: Some of these have been described in the text and in Tables II–IV. The MSS superstable orbits are denoted as M^k, k being the even period. Subscripts denote the different itineraries of the same period. Period-6 superstable MSS line M^6 are shown and those corresponding to other periodic orbits (given in the tables) are not shown here. The non-MSS superstable orbits, which are not allowed from the kneading theory for unimodal maps, are denoted as N^k. $J_\pm^k$ orbits connect the critical points of the maps f_+ and f_- in k steps. The intersection of two such lines gives the DSS orbit. Here D^6 shows the period-6 DSS orbit.

TABLE II. Extended MSS sequences for periodic (with period ≤11) orbits starting from $\varepsilon'=0$ line, between $r=3.569\,946\ldots$ and $r=3.67\ldots$ and then moving up toward the right-hand side in the parameter space for higher ε' values.

Period k	Itinerary	Notation
2	C_R$_+$	$\tilde{M}_1^2$
4	C_R$_+$L_R$_+$	$\tilde{M}_1^4$
8	C_R$_+$L_R$_+$R_R$_+$L_R$_+$	$\tilde{M}_1^8$
10	C_R$_+$L_R$_+$R_R$_+$L_R$_+$L_R$_+$	$\tilde{M}_1^{10}$
6	C_R$_+$L_R$_+$R_R$_+$	$\tilde{M}_1^6$
8	C_R$_+$L_R$_+$R_R$_+$R_R$_+$	$\tilde{M}_2^8$
10	C_R$_+$L_R$_+$R_R$_+$R_R$_+$R_R$_+$	$\tilde{M}_2^{10}$

When these two intersect, this gives the doubly superstable period-6 orbit with the itinerary

$$D^6 \equiv \mathrm{C_+R\_L_+C\_R_+R\_}. \tag{20}$$

Periodic orbits that start from the $\varepsilon'=0$ line and continue for higher ε' values can be classified with the extended MSS algebra, and the corresponding U sequences are listed in Tables II and Table III. There are also the so-called "non-MSS" periodic orbits [26]: These do not continue onto the $\varepsilon'=0$ line and can be seen in Fig. 1. As discussed in other similar modulated systems, such itineraries evolve out of doubly superstable orbits; an example of the period-6 case being

$$N_1^6 \equiv \mathrm{L_+R\_L_+C\_R_+R\_}, \quad \equiv \mathrm{C\_R_+R\_L_+R\_L_+}, \tag{21}$$

$$N_2^6 \equiv \mathrm{R_+R\_L_+C\_R_+R\_}, \quad \equiv \mathrm{C\_R_+R\_R_+R\_L_+}. \tag{22}$$

Note that both these would be forbidden in a single unimodal map (in MSS notation, they are $\mathrm{R^2LRL}$ and $\mathrm{R^4L}$).

The superstable orbits in the parameter space (both the MSS and non-MSS ones listed in Tables II–IV) form the skeleton about which the dynamical behavior in this system is organized as can be seen in Fig. 4. Similar analysis is possible for higher period dichotomous modulation, and we discuss this in the next section.

TABLE III. Extended MSS sequences for periodic (with period ≤11) orbits starting from $\varepsilon'=0$ line, between $r=3.569\,946\ldots$ and $r=3.67\ldots$ and then moving up toward the left-hand side in the parameter space for higher ε' values.

Period k	Itinerary	Notation
2	C$_+$R_	M_1^2
4	C$_+$R_L$_+$R_	M_1^4
8	C$_+$R_L$_+$R_R$_+$R_L$_+$R_	M_1^8
10	C$_+$R_L$_+$R_R$_+$R_L$_+$R_L$_+$R_	M_1^{10}
6	C$_+$R_L$_+$R_R$_+$R_	M_1^6
8	C$_+$R_L$_+$R_R$_+$R_R$_+$R_	M_2^8
10	C$_+$R_L$_+$R_R$_+$R_R$_+$R_R$_+$R_	M_2^{10}

TABLE IV. Notation describing the lines in parameter space. The subscripts on C, R, and L indicate which map, $f_\pm$ determines the dynamics. M^k denotes MSS superstable period-k orbits. $J_\pm^k$ orbits connects the critical points in the two maps ($f_\pm$) and vice versa in k steps. N^k denotes non-MSS superstable period-k orbits.

	Itinerary	Orbit equation
J_+^3	C$_+$R_L$_+$C_	$f_+(f_-(f_+(\frac{1}{2})))=\frac{1}{2}$
J_-^3	C_R$_+$R_C$_+$	$f_-(f_+(f_-(\frac{1}{2})))=\frac{1}{2}$
N_j^6	C_R$_+$R_L$_+$R_L$_+$(j=1)	$f_+(f_-(f_+(f_-(f_+(f_-(\frac{1}{2}))))))=\frac{1}{2}$
	C_R$_+$R_R$_+$R_L$_+$(j=2)	
M_j^6	C$_+$R_L$_+$R_R$_+$R_(j=1)	$f_+(f_-(f_+(f_-(f_+(f_-(\frac{1}{2}))))))=\frac{1}{2}$
	C$_+$R_L$_+$L_R$_+$R_(j=2)	

III. HIGHER PERIOD MODULATION

For higher periods, the two different forms of modulation that we have considered give rise to distinct dynamical systems. The period-3 dichotomous forced map is

$$x_{n+3} = f_+(f_-(f_+(x_n))) \tag{23}$$

while the sinusoidal case becomes

$$\begin{aligned} x_{n+1} &= (r+\varepsilon)x_n(1-x_n), \\ x_{n+2} &= (r-\varepsilon/2)x_{n+1}(1-x_{n+1}), \\ x_{n+3} &= (r-\varepsilon/2)x_{n+2}(1-x_{n+2}), \end{aligned} \tag{24}$$

so that over a period, the modulation averages to zero. We have studied the cases $k=3,4,5$ explicitly, namely periods 3, 5, 8, and in the next section, we consider the limit $k\to\infty$.

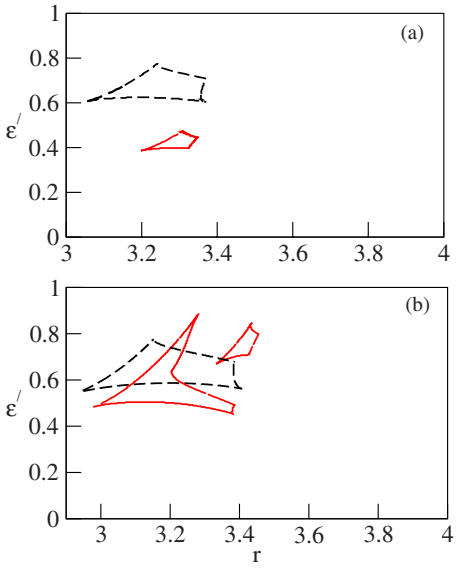

FIG. 5. (Color online) Regions of coexistence for period-3 (dashed line) and period-5 (solid) modulation for (a) dichotomous drive of map compositions $f_{3\beta}$ and $f_{5\beta}$, and (b) sinusoidal drive. In both cases, bistability is observed but for $f_{3\beta}$ and $f_{5\beta}$, tristability is observed.

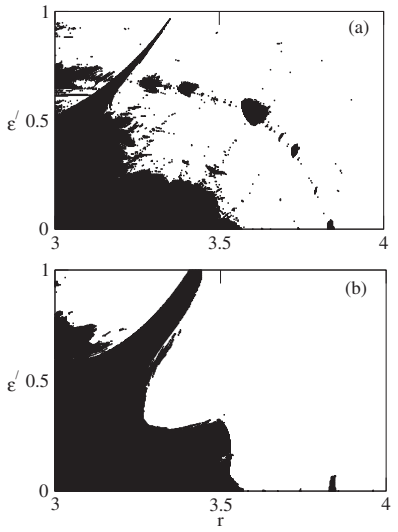

FIG. 6. Dynamical behavior in the limit of quasiperiodic forcing as $k \to \infty$ for (a) dichotomous drive of map $f_{k\beta}$ and (b) sinusoidal drive. The black (white) regions corresponds to stable nonchaotic (chaotic) dynamics. For a sinusoidal drive, strange nonchaotic attractors are formed at the boundaries between regular and chaotic motion.

For the dichotomous modulation, the sign sequences we consider are constructed via concatenation, so that the composite maps are, for example,

$$f_{3\alpha} = f_{2\alpha} \circ f_- \equiv f_- \circ f_+ \circ f_-,$$

$$f_{3\beta} = f_{2\beta} \circ f_+ \equiv f_+ \circ f_- \circ f_+, \tag{25}$$

and

$$f_{5\alpha} = f_{3\alpha} \circ f_{2\alpha} \equiv f_- \circ f_+ \circ f_- \circ f_- \circ f_+,$$

$$f_{5\beta} = f_{3\beta} \circ f_{2\beta} \equiv f_+ \circ f_- \circ f_+ \circ f_+ \circ f_-, \tag{26}$$

respectively. The higher period-m maps $f_{m\alpha}$ ($f_{m\beta}$) can be constructed similarly. For the periods $m = F_k \neq 2$, $f_{m\alpha}$ and $f_{m\beta}$ are not topologically conjugate and the governing dynamics are different.

Period-3 modulation stabilizes the period-3 orbit of the logistic map and its harmonics. This gives rise to a large region of stable period-3 dynamics in parameter space along with its harmonics. In a manner analogous to the period-2 case, tangent bifurcations create an unstable fixed point about which the local maxima and minima are boxable, and multistability results with three coexisting attractors.

Extending this analysis, it can be seen that bistablity for period-m forcing arises when there are tangent bifurcations and the local critical points are boxable about the newly created unstable fixed points. In general, the multistability regions of a map f_m with period-m forcing and its pth composition satisfy the following conditions:

$$f_m^{2p}(x_{cl}) \leq x^*, \quad f_m^{2p}(x_{cr}) \geq x^*, \tag{27}$$

where x^* is the nearest unstable point from the origin about which the left-hand and right-hand critical points (x_{cl}, x_{cr}) are boxable. The regions of multistability in the parameter plane

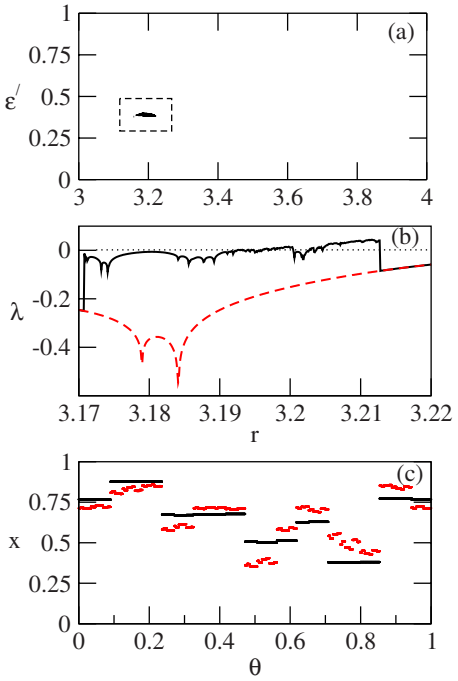

FIG. 7. (Color online) (a) Region of coexistence of attractors in the quasiperiodic limit for dichotomously driven map $f_{k\beta}$ (shown inside the box). (b) Variation of Lyapunov exponents λ with r for characteristic value of ε', here taken to be 0.390 592. (c) The coexisting nonchaotic attractors at $(r = 3.19, \varepsilon' = 0.390\,592)$. The trajectories of the attractors have $\lambda = -0.246\,095$ (black) and $\lambda = -0.014\,128$ [red (dark gray)], respectively.

are bounded by the corresponding iterates of the fixed points of f_m and the transfer crisis loci, as discussed in the case of period 2 above; see Fig. 5.

In general, the area of regions in the parameter plane that support multistability decreases with the period of the modulation, although the variation is not necessarily monotonic. Accurate estimates are difficult to derive since the number of regions increases with the period while their areas decrease with the order.

Interestingly, however, even in the limit of large Fibonacci periods, multistability persists for the dichotomous modulation. We discuss this case below.

IV. QUASIPERIODIC MODULATION

Does bistability (or multistabilty) persist in the limit of aperiodic modulation? In order to address this question, we consider the limit $k \to \infty$ when the rotation, Eq. (3), becomes irrational. As a consequence, the modulated nonlinearity, α_n, becomes aperiodic, and all periodic orbits in the system are destroyed.

Quasiperiodically driven logistic mappings have been studied in considerable detail in earlier work [5] and it is well known that for the case of sinusoidal modulation, strange nonchaotic attractors (SNA) can be created in a measurable region of the parameter space: The motion has nonpositive largest Lyapunov exponent although the attractor is geometrically fractal [4–7]. In this system there is no evi-

dence for the occurrence of bistability (or of multistability).

The situation appears to be different for the case of dichotomous modulation. Shown in Fig. 6 is a characterization of the dynamics as a function of the parameters. As can be seen in Fig. 7, one (fairly large) region of multistability persists for $f_{k\beta}$. (Similarly, the complementary mapping, $f_{k\alpha}$ also has multistability regions but this is not shown here.) However, perhaps owing to the dichotomous nature of the modulation, the dynamics is either chaotic or regular, with no evidence of the strange nonchaotic dynamics [5] that is so characteristic of other quasiperiodically driven dynamical systems.

When the forcing is sinusoidal, multistability vanishes and numerous studies have established that there can be strange nonchaotic attractors (SNAs) near the boundaries of chaotic and nonchaotic regions [5]. Although multistability has been reported in systems where the motion is on SNAs [34], these have been restricted to coupled systems. Multistability has also been reported in the quasiperiodically forced circle map [35].

Here the regions of coexisting attractors also occur in proximity to the boundary between chaotic and nonchaotic dynamics. The coexisting attractors can either be both nonchaotic or one can be chaotic and one nonchaotic; see Fig. 7.

V. DISCUSSION AND SUMMARY

The logistic map is one of the simplest dynamical models within which one can explore the diverse phenomena that occur in nonlinear systems. Most of the dynamical phenomena is characteristic of a wider class of nonlinear systems.

Parametric modulation of the parameters gives rise to new and interesting dynamical behavior, and here we have seen the manner in which multistability arises with periodic modulation of arbitrarily long periods. For the case of period 2, we have given a complete characterization of the manner in which the regions of multistability are organized. These have a complicated and hierarchical structure. We have found the conditions for multistability analytically, and have identified the (parameter) boundaries of such regions. The origins of different multistable regions can be identified; such knowledge could be useful in targeting different basins of attraction to obtain a specific dynamical behavior. Further, we showed that the organization of periodic orbits can be understood via an extension of the results of Metropolis, Stein, and Stein [25]; this scheme helps in rationalizing the different periodic orbits that can arise in such periodically driven systems.

Even with quasiperiodic driving, multistability persists for dichotomous modulation. While this is probably peculiar to the specific form of the drive that we have chosen, the possibility that there can be multistability in other quasiperiodically driven dynamical systems cannot be discounted. It will be interesting to explore whether other dynamical systems share these features.

ACKNOWLEDGMENT

T.U.S. and A.N. acknowledge support from the CSIR, India.

[1] E. Ott, C. Grebogi, and J. A. Yorke, Phys. Rev. Lett. **64**, 1196 (1990).
[2] For a review, see T. Shinbrot, Adv. Phys. **44**, 73 (1995); *Handbook of Chaos Control: Foundations and Applications*, edited by H. G. Schuster (Wiley-VCH, Berlin, 1999).
[3] S. J. Linz and M. Lucke, Phys. Rev. A **33**, 2694 (1986).
[4] C. Grebogi, E. Ott, S. Pelikan, and J. Yorke, Physica D **13**, 261 (1984).
[5] J. F. Heagy and S. M. Hammel, Physica D **70**, 140 (1994); A. Prasad, V. Mehra, and R. Ramaswamy, Phys. Rev. Lett. **79**, 4127 (1997).
[6] T. Yalçinkaya and Y. C. Lai, Phys. Rev. Lett. **77**, 5039 (1996); T. Nishikawa and K. Kaneko, Phys. Rev. E **54**, 6114 (1996).
[7] A. Prasad, S. Negi, and R. Ramaswamy, Int. J. Bifurcation Chaos **11**, 291 (2001); A. Prasad, A. Nandi, and R. Ramaswamy, *ibid.* **17**, 3397 (2007).
[8] H. M. Gibbs, *Optical Bistability: Controlling Lights with Lights* (Academic, Orlando, 1985).
[9] G. P. King and S. T. Gaito, Phys. Rev. A **46**, 3092 (1992).
[10] Y. Du and J. Shi, Trans. Am. Math. Soc. **359**, 4557 (2007).
[11] J. E. Ferrell and W. Xiong, Chaos **11**, 227 (2001).
[12] M. Laurent and N. Kellershohn, Trends Biochem. Sci. **24**, 418 (1999).
[13] J. Hasty, D. McMillen, F. Isaacs, and J. J. Collins, Nat. Rev. Genet. **2**, 268 (2001).
[14] J. Foss, A. Longtin, B. Mensour, and J. Milton, Phys. Rev. Lett. **76**, 708 (1996).
[15] Z. Yi, K. K. Tan, and T. H. Lee, Neural Comput. **15**, 639 (2003).
[16] A. N. Pisarchik and B. F. Kuntsevich, IEEE J. Quantum Electron. **38**, 1594 (2002).
[17] V. N. Chizhevsky, Phys. Rev. E **64**, 036223 (2001).
[18] A. N. Pisarchik and B. K. Goswami, Phys. Rev. Lett. **84**, 1423 (2000).
[19] F. T. Arecchi, R. Meucci, G. Puccioni, and J. Tredicce, Phys. Rev. Lett. **49**, 1217 (1982).
[20] J. Hasty, M. Dolnik, V. Rottschäfer, and J. J. Collins, Phys. Rev. Lett. **88**, 148101 (2002).
[21] M. Schroeder, *Fractal, Chaos, Power Laws* (W. H. Freeman, New York, 1991).
[22] Sanju and V. S. Varma, Phys. Rev. E **48**, 1670 (1993).
[23] S. J. Chang, M. Wortis, and J. A. Wright, Phys. Rev. A **24**, 2669 (1981).
[24] E. Barreto, B. R. Hunt, C. Grebogi, and J. A. Yorke, Phys. Rev. Lett. **78**, 4561 (1997).
[25] M. Metropolis, M. L. Stein, and P. R. Stein, J. Comb. Theory, Ser. A **15**, 25 (1973).
[26] A. Nandi, D. Dutta, J. K. Bhattacharjee, and R. Ramaswamy, Chaos **15**, 023107 (2005).
[27] P. Collet and J. P. Eckman, *Iterated Maps on the Interval as*

Dynamical Systems (Birkhauser, Boston, 1980).
[28] J. A. C. Gallas, Phys. Rev. Lett. **70**, 2714 (1993); Physica A **202**, 196 (1994).
[29] B. R. Hunt, J. A. C. Gallas, C. Grebogi, J. A. Yorke, and H. Koçak, Physica D **129**, 35 (1999).
[30] J. Guckenheimer, F. G. Oster, and A. Ipaktchi, J. Math. Biol. **4**, 101 (1976).
[31] D. Singer, SIAM J. Appl. Math. **35**, 260 (1978).
[32] Y. Yamaguchi and K. Sakai, Phys. Rev. A **27**, 2755 (1983).
[33] J. Testa and G. A. Held, Phys. Rev. A **28**, 3085 (1983).
[34] M. D. Shrimali, A. Prasad, R. Ramaswamy, and U. Feudel, Phys. Rev. E **72**, 036215 (2005).
[35] H. M. Osinga, J. Wiersig, P. Glendinning, and U. Feudel, Int. J. Bifurcation Chaos **11**, 3085 (2001).